Numerical Methods in Civil Engineering, 6-1 (2021) 10-21

Numerical Methods in Civil Engineering

Journal Homepage: https://nmce.kntu.ac.ir/

Seismic Risk Assessment of Optimally Designed Highway Bridge Isolated by Ordinary Unbounded Elastomeric Bearings

Ali Maghsoudi-Barmi[*], Ali Khansefid[**], Alireza Khaloo[***], Milad Ehteshami Moeini[****]

ARTICLE INFO

RESEARCH PAPER

Article history:
Received:
April 2021.
Revised:
June 2021.
Accepted:
July 2021.

Keywords:
Bridge
Fragility function
Seismic performance
Risk assessment
Unbounded elastomeric bearings

Abstract:

Recent experimental research has shown that ordinary unbounded steel reinforced elastomeric bearings (SREBs) can be considered as an attractive cost-effective option for the seismic isolation of highway bridges. To further investigate its benefits, the current study is focused on the seismic risk assessment of an optimally designed highway bridge isolated by SREB system. A typical three-span highway bridge located in Tehran Metropolis is considered and designed with the SREBs as isolation system, applying a multi-objective optimization procedure to reduce both the seismic isolation deformation and the base shear, simultaneously. Then, the vulnerability of the bridge is evaluated through an Incremental Dynamic Analysis (IDA) using a suite of 20 ground motion records, and the fragility functions are generated. Next, for the hazard modelling, all active faults around the site of the project are taken into account to simulate the earthquake scenario. Afterwards, probable earthquake scenarios during the design life of the bridge are generated randomly, including the events, as well as their corresponding synthetic stochastic accelerograms. In the last step, the response of the bridge and its losses are calculated under the entire scenarios. Finally, the seismic risk of the bridge is estimated. The results indicate an improved behavior of the bridge, and the capability of isolation system in mitigating the earthquake excitation. Moreover, the results, obtained from the assessed seismic risk, show a significant reduction in the amount of bridge losses.

1. Introduction

Seismic isolation is amongst the most effective methods to reduce the probable seismic induced structural damages. However, commonly used seismic isolators are generally too expensive, which led to a series of studies on optimal low-cost seismic isolators. Natural rubber elastomeric bearings reinforced with steel shims, which are currently popular as bearings for service loads at bridges, are one of the firsts in line as low-cost isolators. Many have sought to investigate the inherent capabilities of steel-reinforced elastomeric bearings (SREBs) to provide improved structural performance under seismic excitations [1-5].

* *PhD, Department of Civil Engineering, Sharif University of Technology, Tehran, Iran.*
** *Assistant Professor, Department of Civil Engineering, KN Toosi University of Technology, Tehran, Iran.*
*** *Corresponding author: Professor, Department of Civil Engineering, Sharif University of Technology, Tehran, Iran. Email: khaloo@sharif.edu.*
**** *MSc, Department of Civil Engineering, University of Science & Culture, Tehran, Iran.*

SREBs can be divided into three categories regarding connection to superstructure and substructure. The first type includes rigid connection of both upper and lower surfaces of the bearing to superstructure and substructure using thick endplates, which is considered as bounded. Next one uses frictional contact at the upper and lower surfaces of the bearing and is considered as unbounded. The combination of the two configurations is also possible as the third type. Of the three types of configurations mentioned, the unbounded type brings advantages by reducing the tensile stress. Furthermore, they are cheaper compared to bounded bearings due to elimination of thick endplates which also require the expensive vulcanization technique [6]. Behavior of ordinary elastomeric bearings under seismic excitation has been experimentally investigated by some researchers in the past. Mori et al. [1] conducted extensive experiments on unbounded elastomeric bearings to assess the shear response. These experiments were carried out up to shear strain of 200% of total rubber height. In another study

conducted by Konstantinidis et al. [2] it was proved that ordinary steel reinforced elastomeric bearings possess adequate lateral displacement capacity and can be used as a seismic isolation system. In another recent study, Steelman et al. [3] investigated shear and friction response of non-seismic laminated elastomeric bridge bearings subjected to seismic demands. Maghsoudi-Barmi et al [4] presented an experimental program to analyze the mechanical properties of steel-reinforced natural rubber bearings without the upper and lower endplates when subjected to large shear displacements, and to assess how they can be used and what the limitations are. In another study, Maghsoudi-Barmi and Khaloo [5] studied the lifetime performance of the ordinary elastomeric bearings as an isolation system. Other than the several experimental studies, numerical investigations were also carried out to develop a practical bilinear model capable of simulating the cyclic behavior of the SREBs while considering the interaction of axial and shear loads [7].

All the previously mentioned studies have one aspect in common, which is cost effectiveness of the proposed isolation system as well as the inherent capacity to reduce seismically induced forces transmitted to the substructure.

Previous studies have been carried out while considering critical parameters. However, they are mostly micro scale and only consider the overall performance of the bearing. Therefore, additional research is needed regarding the probabilistic assessment of the seismic performance of a bridge equipped with the introduced system and also to estimate the seismic risk of the bridge under investigation. For this purpose, a three-span highway bridge was chosen and designed while a multi objective optimization procedure was employed to reduce the seismic isolation deformation and the induced base share. Nonlinear incremental dynamic analyses (IDA) were performed to generate fragility functions using a set of 20 ground motions. Afterward, probable earthquake scenarios during the design life of the bridge were generated randomly, including the events, as well as their corresponding synthetic stochastic accelerograms. In the last step, response of the bridge and its losses were calculated under the entire scenarios, and the seismic risk of the bridge was estimated.

2. Bridge model

2.1 Bridge geometry

Figure 1 shows the overall geometry of the studied bridge, which is a typical three span continuous bridge located in a seismically high-level region (S_{DS}=1.231, S_{D1}=0.508, and A_s=0.502). The outer and the middle spans are 20 m and 30 m, respectively. A voided slab system with width of 14.3 m and height of 1.4 m was considered as the bridge deck. This bridge is considered in two cases of connections between the Piers and the deck including fixed connection, and unbounded isolated. The bearing geometrical and material properties are listed in Table 2. The bearing dimensions were chosen using a multi objective optimization procedure, reducing the seismic isolation deformation and the induced base shear (described in the upcoming sections). The bridge contains two circular column piers with a diameter of 1.5 m at two rows spacing 5.7 m from each other. Forty-five longitudinal bars with 32 mm diameters and circular stirrups with 12 mm diameters with a spacing of 100 mm were considered for pier reinforcement. The Un-isolated bridge contained stronger columns with a diameter of 1.6 m and reinforcement of 50 longitudinal bars with diameter of 32 mm, due to larger shear force demand of the substructure. Per As for the soil type, type C of AASHTO LRFD bridge design specifications [8] was considered, meaning that V_s is between 366 m/s and 732 m/s.

2.2 Model Parameters

Nonlinear three-dimensional bridge models were developed in finite element software SAP 2000. The overall analytical model is depicted in Figure 2.

The deck was modeled using a frame element to reduce calculation costs. The columns were also modeled using fame elements incorporating the Mander [9] model which considers the concrete reinforcement. The plastic hinge length was calculated using the proposed model by Berry et al. [10] for bridge pier columns.

To fully incorporate the hysteretic behavior and energy dissipation of the SREBs, relations proposed by Khaloo et al. [7] were used to calculate the corresponding bilinear model. The bilinear model and the associated properties are displayed in Figure 3. The relations (1) to (6) were used to calculate the required parameters.

$$\Delta_n = \alpha \times t_r \tag{1}$$

$$K_I = 3.22 \times \frac{GA}{t_r} \tag{2}$$

$$K_S = (\beta + \theta) \times \frac{GA}{t_r} \tag{3}$$

$$\alpha = 0.01 \times (0.0823 \times \frac{\sigma_V\ (\text{MPa})}{2.18\ (\text{MPa})} \times (\frac{14.79}{S})^{1.3} + 3.75) \tag{4}$$

$$\beta = 0.0016 \times S \times \frac{\sigma_V\ (\text{MPa})}{2.18\ (\text{MPa})} \tag{5}$$

$$\theta = 1.0315 - 0.025 \times \frac{\sigma_V\ (\text{MPa})}{2.18\ (\text{MPa})} \tag{6}$$

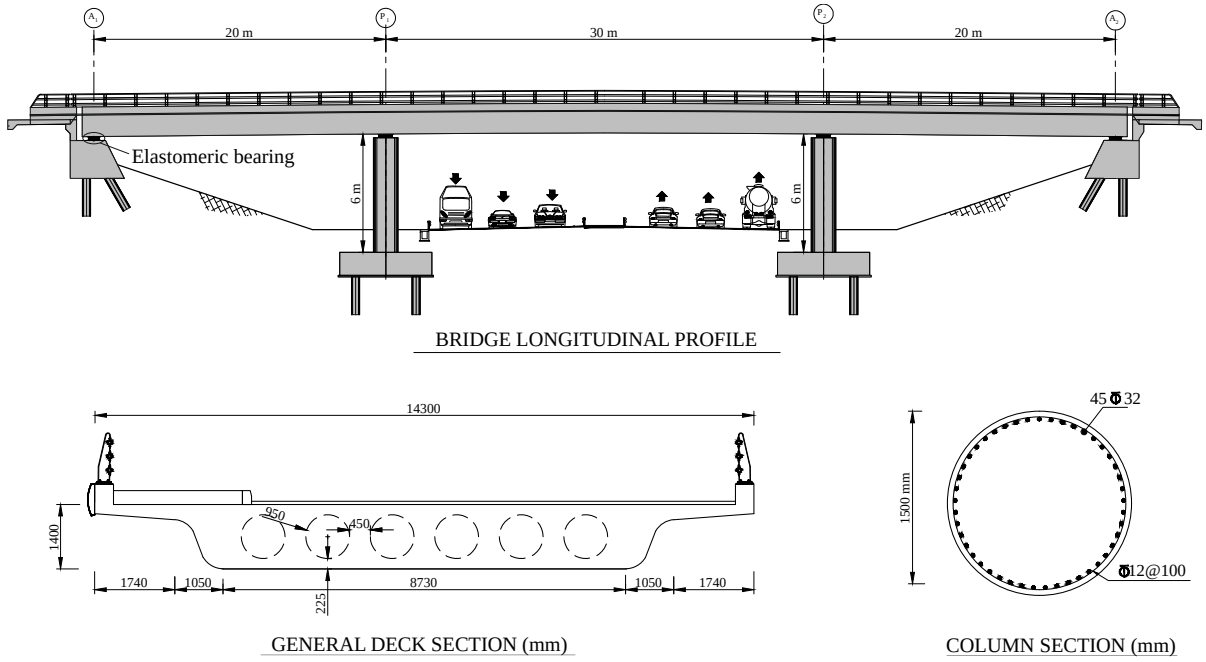

Fig. 1: Overall view of the bridge.

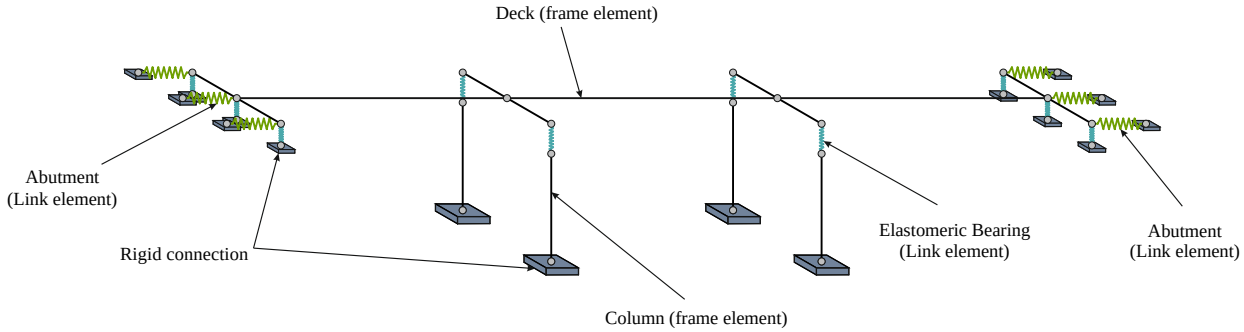

Fig. 2: Schematic of the analytical model.

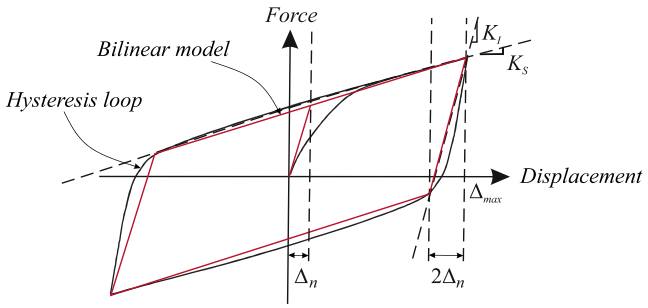

Fig. 3: Bilinear hysteretic model for SREB [7].

One of the most important factors in the bridge response is the soil-structure interaction (SSI). Chaudhary et al. [11] studied the influence of SSI and their studies showed that this parameter can only be a governing effect in soft soils. Therefore, since a dense soil type, i.e., type C, was considered for this study, SSI can be neglected herein.

Quad-linear model proposed by Nielson [12], which is based on Caltrans recommendations [13 and 14] (Figure 4), was used to simulate the back-wall stiffness and the passive soil pressure on the abutment. The definitions and relations as well as the corresponding values are listed in Table 1.

Besides all the attention made regarding the providing an exact numerical model, it should be noted that a numerical model is always affected by model and aleatory uncertainties that influence the structural safety of structural systems.

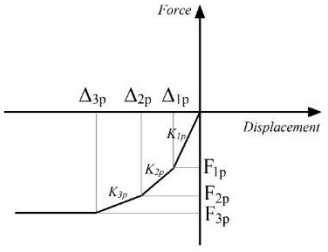

Fig. 4: Analytical model of abutment back-wall in longitudinal direction.

Table. 1: Relationships and the corresponding values for abutment-soil behavior parameters [12]

Parameter	Proposed relation	Values used for this study
K_{1p}	$11.5 - 28.5\ kN/mm$/m	20.2 kN/mm/m
K_{2p}	$\frac{0.55(F_{3p} - F_{1p})}{0.25\Delta_{3p}}$	5.73 kN/mm/m
K_{3p}	$\frac{0.45(F_{3p} - F_{1p})}{0.65\Delta_{3p}}$	1.8 kN/mm/m
F_{1p}	$K_{1p}\Delta_{1p}$	282.8 kN/m
F_{2p}	$F_{1p} + 0.55(F_{3p} - F_{1p})$	483.4 kN/m
F_{3p}	$(0.37\ MPa)h$	647.5 kN/m
Δ_{1p}	$0.10\Delta_{3p}$	14 mm
Δ_{2p}	$0.35\Delta_{3p}$	49 mm
Δ_{3p}	$\left(0.06 + \left(\frac{K_{1p} - 11.5}{28.8 - 11.5}\right)(0.04)\right)h$	140 mm

2.1. Optimal design of base isolation system

The isolation system in this study was designed using the proposed simplified method AASHTO Guide Specifications for Seismic Isolation Design [15]. Lateral deformation and shear force of the isolation units are controlling objectives in the design process of the isolators. Various types of multi objective optimization methods can be used, e.g., criterion based, aggregated-based, and Pareto front [16]. The latter is selected for this study since it is more commonly used for vibration control systems and contains fewer limitations compared to the other methods [17-19]. Furthermore, this method can lead to a set of non-prior optimal results [20]. Although additional criterions are required, this option can allow the engineers to find an optimal solution among the set of obtained results. Amongst several available tools, for e.g., multi objective generic algorithm, costly global optimization, etc., the first was used [21-22]. An important parameter in this method is the number of optimization generations considered as 1024 for this study, as the result of a sensitivity analysis considering 1024, 512 and 256 as the number of generations.

An additional criterion for selecting the final optimal design, i.e., the material quantity (cost of the isolation system) was implemented, which will lead to the cheapest yet effective isolation system for the investigated bridge in this study. The optimal Pareto front of the optimization objectives of the seismically isolated bridge is displayed in Figure 5. The mechanical properties of the selected SREBs are reported in Table 2. The maximum deformation demand was obtained as equal to 0.23 m.

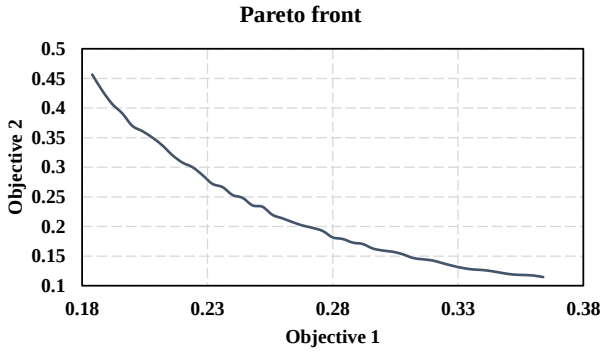

Fig. 5: Optimal Pareto front of the optimization objectives of the seismically isolated bridge.

Table. 2: Characteristics of the optimally designed bearings

Plan dimensions (mm)	900×900
Total thickness (mm)	309
Total elastomer thickness (mm)	239
Number of 18 mm elastomeric layers	13
Number of 5 mm steel-shims	14
Cover layers thickness (mm)	2.5
Shape factor	12.5
Initial Stiffness, kN/m	9821
Secondary Stiffness, kN/m	3050
Characteristic strength, kN	66.3

3. Fragility Function Development methodology

3.1. Definition of the models and parameters

The list of the studied models is presented in Table 3. The model number 1 is defined as isolated bridge using unbounded bearings, meaning that the deck and bearings only have frictional contact with each other. The friction

coefficient of this model is assumed as 0.4 per recommendations of Caltrans manual [23]. To reach a more comprehensive understanding of the proposed isolation system performance, another distinct model was developed with a fixed type connection.

Table. 3: Introduction of generated analytical models

Model	Type of isolation	Notes
Isolated-UB0.4	Unbounded	Friction coefficient of 0.4
Un-isolated	-	Un-isolated bridge model

3.2. Ground motions and intensity measures

The incremental dynamic analysis (IDA) method by using a nonlinear time history analysis is adopted as the analytical method for this research. So, an appropriate number of earthquake records should be selected. The ground motions were specifically chosen to reflect the geotechnical characteristics of the project site as recommended by AASHTO LRFD bridge design specifications [8].

To fulfil this criterion, the soil type matching the soil type C is chosen, with the site-to-source distance varying between 10 and 50 km, the magnitude ranging from 5 to 7.5, and finally, all the records possessing significant spectral acceleration in the period range of the studied bridge.

A set of 20 ground motion records were chosen from the NGA-West2 database provided by the Pacific Earthquake Engineering Research Center. The records' characteristics are provided in Table 4, and the corresponding response spectra, along with the average response, are depicted in Figure 6 for all of the three orthogonal directions. The orthogonal components (x, y, and z) of the selected ground motions are applied to the bridge models, simultaneously.

Fragility functions show the probability of exceeding the predefined performance state of the seismic demand under a specific intensity measure (IM), which represents the seismic loading [24]. Meaning that the selection of an appropriate IM has an important role in reflecting the level of the seismic loading properly.

Some of the proposed spectral acceleration IMs are: (S_a) or (S_d) at the natural vibration mode period, peak ground acceleration (PGA), peak ground velocity (PGV), peak ground displacement (PGD), and Arias intensity (AI). In a related study, Mackie and Stojadinovic [25] investigated 65 different IMs to determine the optimal IM based on practicality, effectiveness, efficiency, sufficiency, and robustness, which were categorized in three classes. They proposed S_a, and S_d at the fundamental period as the ideal IMs. On the other hand, Padgett and DesRoches [26] suggested PGA as the efficient, practical, and most sufficient IM.

The linear correlation of the logarithmic results can be proper acceptance and practicality index to find IM for fragility function generation [25]. Therefore, PGA, PGV, PGD, AI, S_a, and S_d at the fundamental vibration mode of the isolated bridge are considered as IMs. The results are compared in Figure 7. As it is shown in this figure, a strong correlation exists for S_a and S_d, while the weakest correlation can be observed for PGA. Thus, S_d at the fundamental natural vibration mode of the bridge is chosen as the IM to develop the fragility curves.

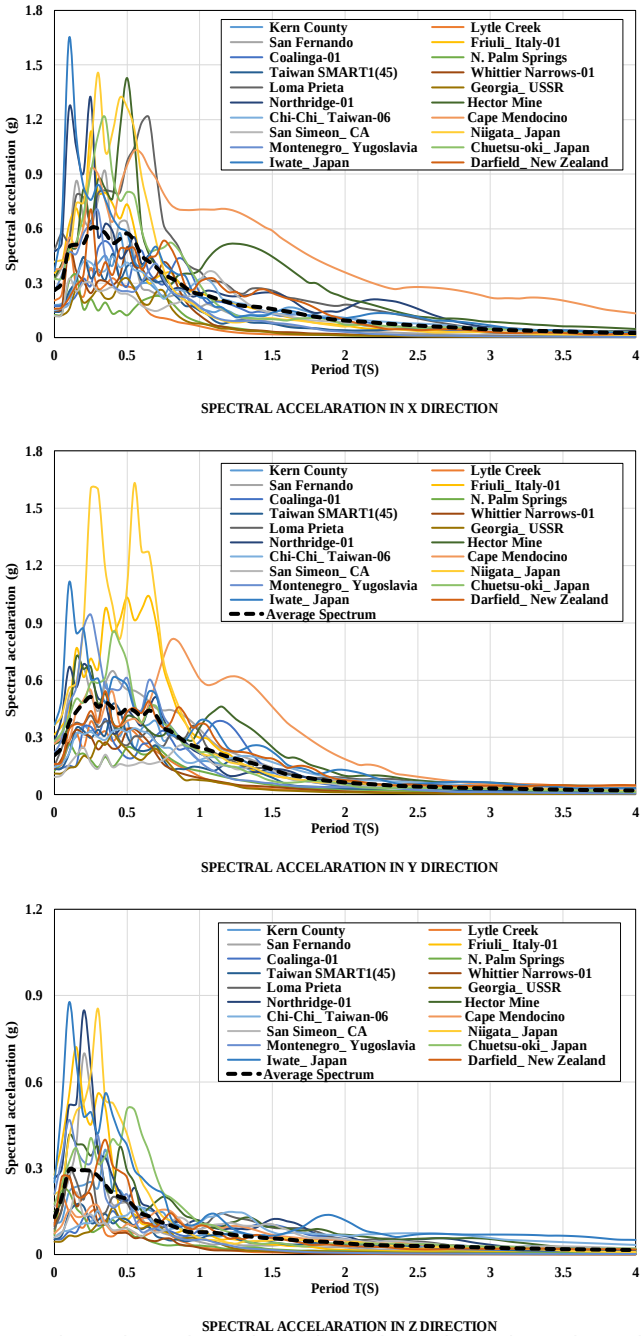

Fig. 6: Response spectra of the selected records for three orthogonal directions of (a) longitudinal, (b) transverse, and (c) vertical.

Table. 4: Characteristics of the selected ground motions.

No.	Event	Year	Station	Magnitude	PGA (g)
1	Kern County	1952	Taft Lincoln School	7.36	0.18
2	Lytle Creek	1970	Wrightwood - 6074 Park Dr	5.33	0.20
3	San Fernando	1971	Castaic - Old Ridge Route	6.61	0.32
4	Friuli_ Italy-01	1976	Tolmezzo	6.5	0.36
5	Coalinga-01	1983	Slack Canyon	6.36	0.17
6	N. Palm Springs	1986	Fun Valley	6.06	0.13
7	Taiwan SMART1(45)	1986	SMART1 E02	7.3	0.14
8	Whittier Narrows-01	1987	La Crescenta - New York	5.99	0.15
9	Loma Prieta	1989	Coyote Lake Dam - Southwest Abutment	6.93	0.48
10	Georgia_ USSR	1991	Iri	6.2	0.12
11	Northridge-01	1994	LA - UCLA Grounds	6.69	0.47
12	Hector Mine	1999	Hector	7.13	0.33
13	Chi-Chi_ Taiwan-06	1999	CHY028	6.3	0.15
14	Cape Mendocino	1992	Ferndale Fire Station	7.01	0.38
15	San Simeon_ CA	2003	San Antonio Dam - Toe	6.52	0.12
16	Niigata_ Japan	2004	NIGH06	6.63	0.42
17	Montenegro_ Yugoslavia	1979	Herceg Novi - O.S.D. Paviviv	7.1	0.26
18	Chuetsu-oki_ Japan	2007	Joetsu Yanagishima paddocks	6.8	0.33
19	Iwate_ Japan	2008	AKT023	6.9	0.37
20	Darfield_ New Zealand	2010	SPFS	7	0.16

3.3. Damage states

Composite deck-girder system, bridge piers and isolation bearings are the most probable components to enter the nonlinear range of deformations under strong seismic excitations in seismically isolated highway bridges [27]. Engineering demand parameters (EDP), which are used to measure the damage state (DS) of the bridge components, have different definitions. The commonly used damage measures for bridge piers are curvature ductility, displacement ductility, and residual displacement, while shear strain, drift ratio, and lateral deformation are common for elastomeric bearings. Herein, four damage states (DS) defined by HAZUS [28] are generally adopted, i.e. slight, moderate, extensive, and collapse damages.

In this study, the defined curvature ductility of the pier column, by Choi et al. [29], is chosen as the corresponding damage index. Base isolation bearing systems usually experience large shear deformations, causing damage to the isolator units and also other structural components. Pounding and unseating issues are also considered as damage states as well as other probable cases which can be defined using experimental programs. Based on the suggestion made by Zhang and Huo [30], the shear strain of the bearing is considered as a damage index in this research; since it can describe the bearing behavior due to the direct dependence of the shear modulus and damping of rubber on shear strain [31], while considering the bearing geometry [30]. Results of experimental studies have shown that modern isolation bearings can experience shear strain up to 400% before rupture or total failure. However, such large shear strain can cause significant deformations which can cause pounding or significant unseating of the deck [30]. Hence, the shear strain of 250% is considered as final damage state in this study. Damage states are defined based on HAZUS [28], and listed in Table 5 with the corresponding damage indexes for different components.

4. Risk assessment methodology

The proposed methodology by Hazus [28] is used to assess the seismic risk of the project. Hazus [28] defines losses in four categories, namely, direct economic losses, direct social losses regarding casualties, direct social losses regarding population displacement and shelter needs, and indirect economic losses.

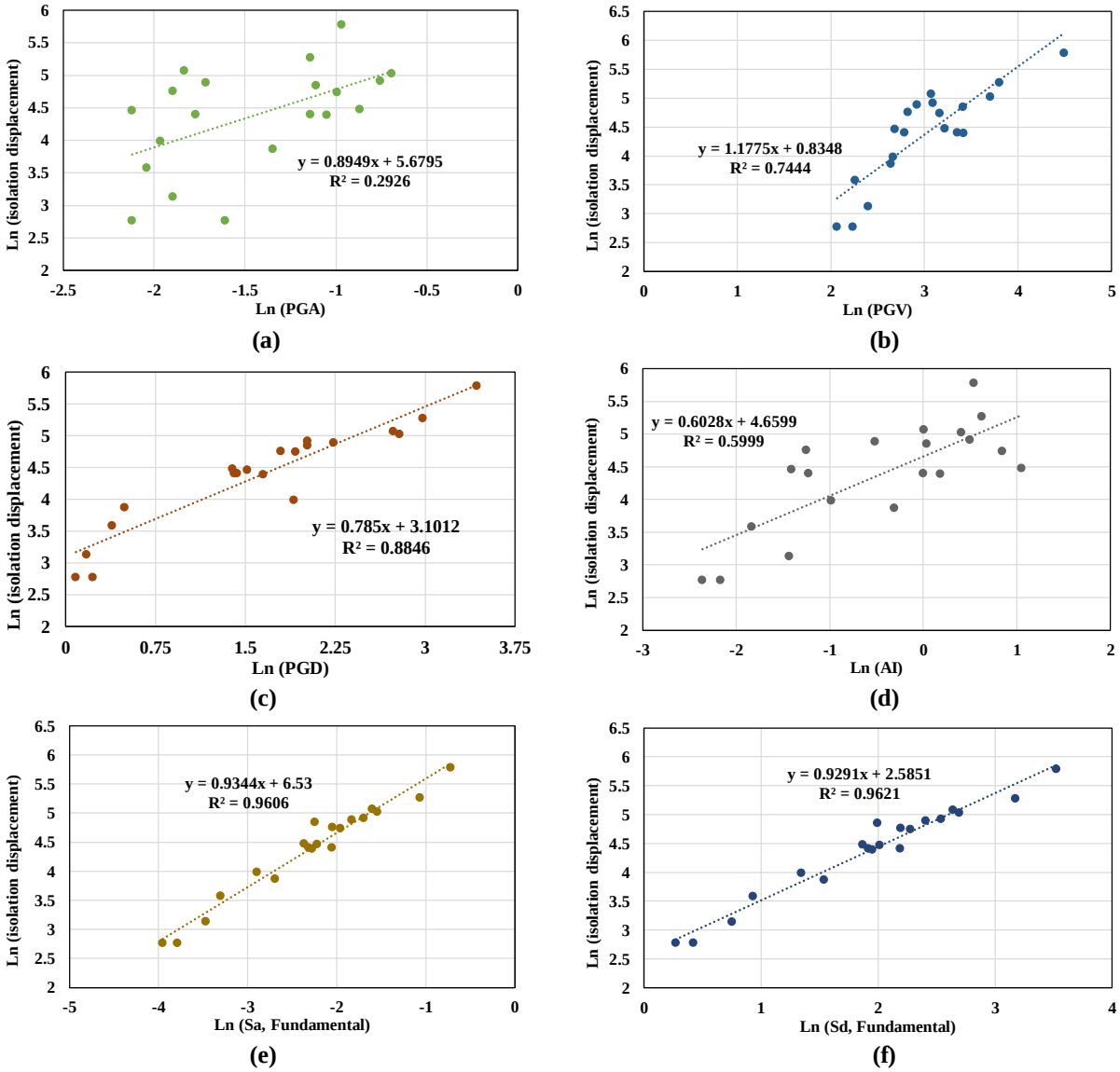

Fig. 7: Comparison of correlation of the results for various IMs.

Table. 5: Corresponding DSs for concrete columns and bearings.

Component	EDP	Damage States			
		Slight (DS=1)	Moderate (DS=2)	Extensive (DS=3)	Collapse (DS=4)
Column	Curvature ductility	1	2	4	7
Elastomeric Bearing	Shear strain	100%	150%	200%	250%

Direct economic losses for each damage state are expressed as a fraction of the bridge replacement cost as shown in Table 6. Regarding the direct social losses due to casualties, the methodology assumes casualty rates for the complete damage state (DS=4) only, considering casualty severity level 4. The casualty rates are shown in Table 7. Direct social losses regarding population displacement and shelter needs do not include bridges and is related to building structures. Lastly, the indirect economic losses were not considered in this research due to the lack of information in this regard.

Table. 6: Damage Ratios for Highway bridge.

Damage State	Damage Ratio
DS=1	0.03
DS=2	0.08
DS=3	0.25
which is DS=4	0.67

Table. 7: Casualty Rates by Specific Bridge Type for Complete Structural Damage

Bridge Type	Casualty Severity Level (%)			
	Severity 1	Severity 2	Severity 3	Severity 4
Major Bridge	17	20	37	7
Continuous Bridge	17	20	37	7
S.S. Bridge	5	25	20	5

4.1. Ground Motion

There are several active faults around the Tehran metro city where the bridge is assumed to be located in. 12 main faults exist in a radius of 100 km around the bridge location as shown in Figure 8, and the main properties of these faults are presented in Table 8 [32]. Each of these faults may be activated in the future based on their triggering probability, which is proportional to their seismicity rate obtained from previous studies [33].

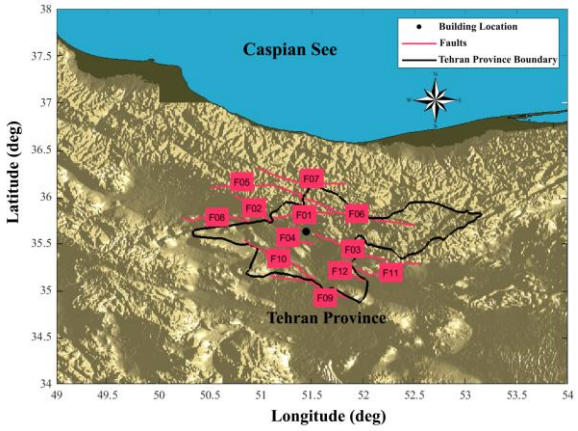

Fig. 8: Map of active faults in Tehran greater area.

Simulation of the earthquake hazard is done randomly using the methodology proposed by Khansefid and Bakhshi [34] for generating random earthquake mainshock-aftershock scenarios, including the seismological properties of events, as well as their corresponding accelerograms. However, aftershocks are not considered in this paper. According to this approach, in the first step, a fault is randomly selected based on their triggering probability. Then, a random event scenario compatible with the conditions of the Iranian plateau is developed containing mainshocks and aftershocks. Afterward, for each of the procreated events, a corresponding synthetic stochastic accelerogram is generated, which is compatible with the condition of the Iranian plateau [35].

Using the aforementioned approach, a total of 6000 earthquake scenario realizations are generated. The statistical properties of developed event scenarios are shown in Figure 9. The magnitudes of mainshocks are from 5 to 9. The focal depth of events varies from 15 km to 30 km, and the site-to-source distance of all events starts from 14 km and goes up to 100 km.

5. Results and discussion

5.1. Fragility Curve Development

The defined models are analyzed while considering the aforementioned conditions, and the corresponding fragility curves are then developed and compared. The results obtained are discussed in this section.

It is assumed that the bridge operates like a serial system containing different components, playing a key role in a way that the damage of each component will result in the bridge damage at the same level. In this case, the overall damage state is calculated as the largest damage state at the component level.

$$DS_{Bridge} = \max(DS_{pier}, DS_{Bearing}) \quad (7)$$

Previous studies [36] have shown that for the isolation system under investigation, the isolation system itself is more vulnerable in comparison with the bridge pier. Therefore, the fragility curves significantly differ, especially in the two first damage states. Accordingly, the whole bridge fragility curves completely coincide with the bearings' fragility curves.

Fragility curves generated for the isolated bridge, along with the Un-isolated bridge, are shown in Figure 10. The most important finding herein is regarding the remarkable performance of the introduced seismic isolation system and the improved response which can be provided in comparison with the Un-isolated bridge. This is shown/presented for all DSs. As displayed, elastomeric bearings managed to drastically decrease the seismic vulnerability of the bridge.

For a more precise investigation, the probability of exceeding different DSs at anticipated levels of earthquakes, which is assumed for this project, namely Service Level Earthquake (SLE, $S_d(T_f)$=0.07m), Design Basis Earthquake (DBE, $S_d(T_f)$=0.23m) and Maximum Considered Earthquake ($S_d(T_f)$=0.37m), are compared in Table 9.

DBE is assumed to have a seven percent probability of exceedance in the life of a bridge at 75 years seismic hazard return period. MCE and SLE have return periods of approximately 2500 years and 100 years, respectively. As it is shown in Table 6, in all DSs for all levels of earthquakes, the vulnerability of the unbounded system is significantly higher than the Un-isolated bridge. This difference increases in damage states of DS=3 and DS=4, which shows that the isolation system has improved the performance of the bridge accordingly in an extreme seismic event.

Table. 8: Characteristics of active faults around Tehran [32].

ID	Fault name	Length (km)	M_{min}	M_{max}	Triggering Probability
F01	North Tehran 1	72.2	5.5	7.2	0.0429
F02	North Tehran	46.9	5.5	7.0	0.0270
F03	Eyvanekey	82.1	5.5	6.9	0.0173
F04	Kahrizak	36.7	5.5	6.8	0.0273
F05	Taleghan	74.0	5.5	6.9	0.0421
F06	Mosha	155.7	5.5	7.6	0.0341
F07	Kandovan	97.2	5.5	7.3	0.0212
F08	Eshtehard	74.7	5.5	7.2	0.0297
F09	Siahkooh	86.8	5.5	7.2	0.0239
F10	Robat Karim	84.4	5.5	7.3	0.0209
F11	Garmsar	76.5	5.5	7.3	0.0328
F12	Pishva	35.3	5.5	7.5	0.0173

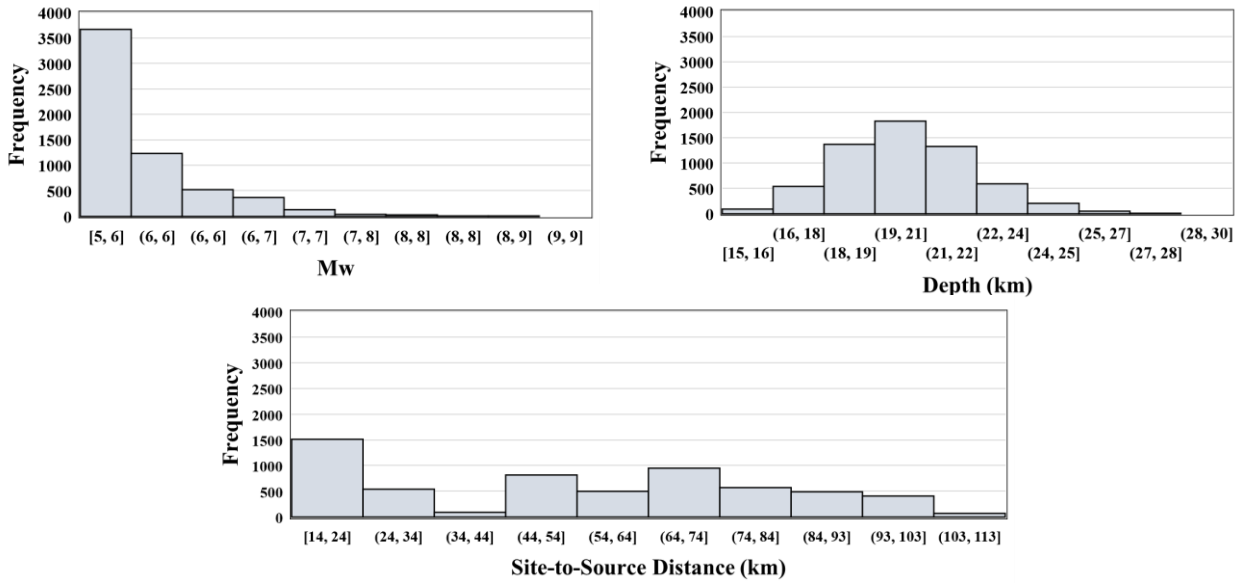

Fig. 9: Statistical properties of major characteristics of generated random events in all scenarios for earthquakes.

Table. 9: Probability of exceedance of different damage states for bounded and unbounded bearings at SLE, DBE and MCE earthquake levels.

Earthquake Level	DS=1		DS=2		DS=3		DS=4	
	Isolated-UB0.4	Un-isolated	Isolated-UB0.4	Un-isolated	Isolated-UB0.4	Un-isolated	Isolated-UB0.4	Un-isolated
SLE	0	0.82	0	0.55	0	0.24	0	0.07
DBE	0.53	1	0.08	1	0.02	0.9	0.02	0.69
MCE	0.98	1	0.58	1	0.29	1	0.18	0.9

5.2. Risk assessment

A total of 6000 random earthquake scenarios were generated using the Mont-Carlo simulation approach, and the response of the structure was evaluated under these scenarios to calculate the seismic risk of the introduced seismic isolation system. Figure 11 illustrates the loss curve generated for the bridge, in both cases of isolated and Un-isolated bridges. As it is shown, the spectral displacement of generated earthquake scenarios at the fundamental period of the structure, is below 0.5 m.

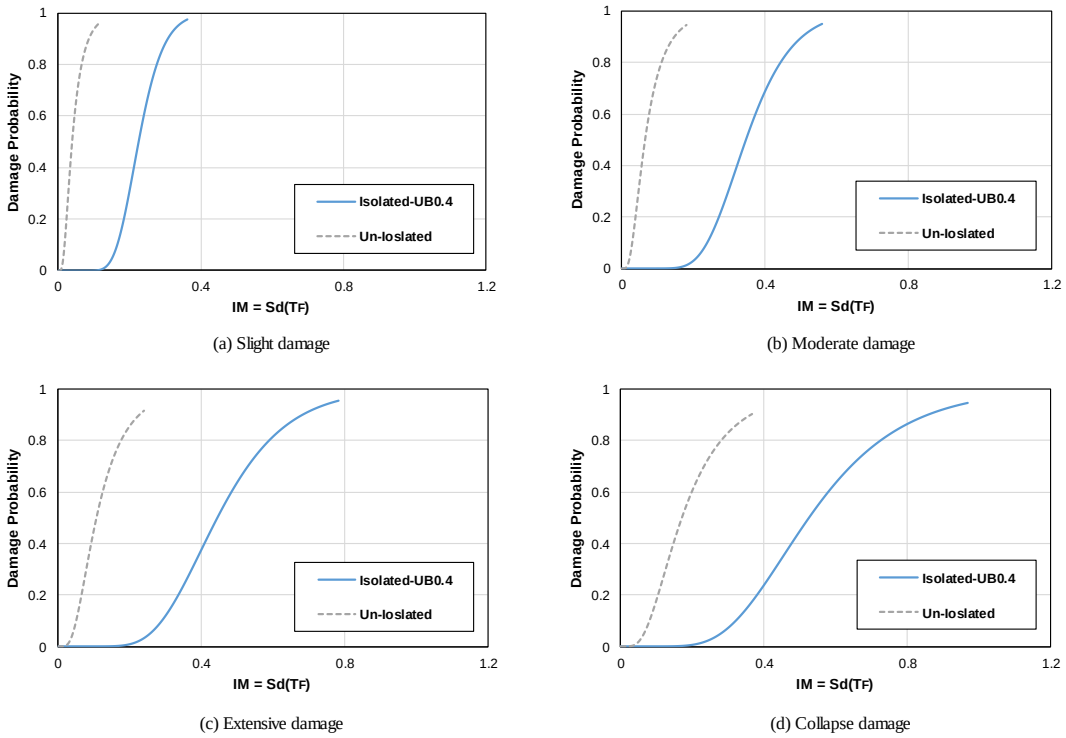

(a) Slight damage (b) Moderate damage

(c) Extensive damage (d) Collapse damage

Fig. 10: Comparison of fragility Curves for Isolated and Un-isolated models.

Looking through Figure 10, regarding the fragility curves developed for the bridge, we can say that the possible earthquake in the location of the project, is not strong enough to create severe damage corresponding to state DS4. Therefore, the total loss which is generated in the bridge is just due to direct economic losses and no loss from casualty has occurred, since the methodology assumes casualty rates for the complete damage state (DS4) only. As it is shown in Figure 11, the loss to the bridge has dramatically decreased by using elastomeric bearings as isolation system. Considering different anticipated levels of earthquakes, which is assumed for this project, namely Service Level Earthquake (SLE, $S_d(T_f)$=0.07m), Design Basis Earthquake (DBE, $S_d(T_f)$=0.23m) and Maximum Considered Earthquake (MCE, $S_d(T_f)$=0.37m), a better comparison can be presented. In the presence of SLE, loss to the bridge is almost equal to zero in the isolated bridge, while it is 11% for the Un-isolated bridge. This difference is higher in the DBE level earthquake, in which the total loss of 23.2% has decreased to 2.6% by using seismic isolation system. Lastly, when MCE level earthquake occurs, losses of 11.8% and 24.2% can be anticipated for Isolated and Un-isolated bridges.

The probability of exceedance estimates for the bridge loss is also depicted in Figure 12. As it is shown in this figure, using seismic isolation system has resulted in remarkable reduction in the estimated probability of bridge loss in which, losses over 10% in the isolated bridge is almost seldom for the location under investigation, while a probability level of 45% is estimated for Un-isolated bridge.

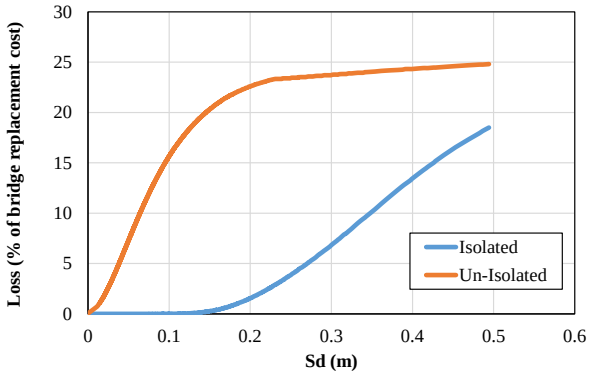

Fig. 11: Loss curve for Isolated and Un-isolated bridges.

Seismic isolation system has proven to be a structural system, which can dramatically enhance the response of the bridge to seismic isolation through the shift period and the consequent reduction in the seismic force induced in the structure. Moreover, the damage to the structure mainly concentrate on fuse type elements named seismic isolators, and depending on their abilities, less damage is caused to the bridge structure. Interestingly, a similar trend was also visible in the bridge equipped with the introduced seismic isolation system, and the seismic risk of the bridge for isolated bridge was remarkably evaluated less than Un-isolated bridge.

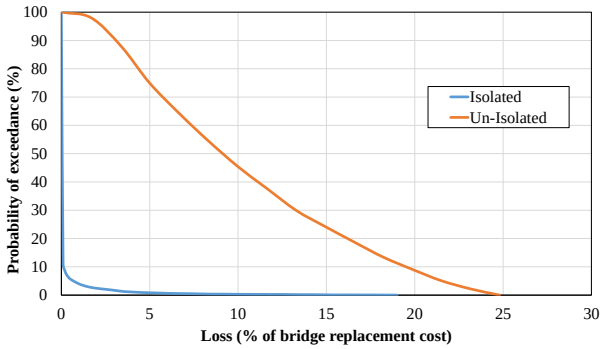

Fig. 12: probability of exceedance estimates for Loss.

6. Conclusion

Probabilistic seismic performance assessment of an optimally designed bridge isolated by ordinary unbounded laminated elastomeric bearings was investigated through developing fragility curves. The seismic risk of the bridge was also estimated using Hazus [28] methodology. The main concluding remarks of this research can be summarized as of the followings.

1. Considering the linear correlation of the results in a logarithmic form, spectral displacements at the fundamental period of the structure (S_d) were shown to be the most appropriate IM for assessing the seismic performance of the isolated bridge with SREBs.
2. Assuming that the bridge operates like a serial system including different components, the isolation system was shown to be significantly more critical in comparison with the pier columns and controls the fragility curve obtained for the whole bridge.
3. Using unbounded laminated elastomeric bearings as an isolation system decreased the probability of exceedance of all defined DSs dramatically. This proves an appropriate seismic performance for this type of isolation system, even for severe earthquakes.
4. For the project investigated in this paper, the loss to the bridge has dramatically decreased by using elastomeric bearings as isolation system. Using seismic isolation system has made a remarkable reduction in the probability of the loss on the bridge over a 50-year life of the project.

References:

[1] A. Mori, P. J. Moss, N. Cooke, and A. J. Carr, The behavior of bearings used for seismic isolation under shear and axial loa, Earthq Spectra, 15 (1999), 199-223.

[2] D. Konstantinidis, M. JAMES, J. M. Kelly, and N. MAKRIS, Experimental Investigation on the Seismic Response of Bridge Bearings, Report 2008/02. Earthquake Engineering Research Center, University of California, Berkeley, 2008.

[3] J. Steelman, L. A. Fahnestock, E. T. Filipov, J. M. LaFave, J. F. Hajjar, and D. A. Fouch, Shear and Friction Response of Nonseismic Laminated Elastomeric Bridge Bearings Subject to Seismic Demands, J Bridge Eng, 18 (2013), 612-623.

[4] G. Wu, K. Wang, G. Lu, and P. Zhang, An Experimental Investigation of Unbonded Laminated Elastomeric Bearings and the Seismic Evaluations of Highway Bridges with Tested Bearing Components, Shock and Vibration, Volume 2018 (2018), 18 pages.

[5] A. Maghsoudi-Barmi, A. Khaloo, Experimental investigation of life-time performance of unbounded natural rubber bearings as an isolation system in bridges, Structure and Infrastructure Engineering, Online Published (2020), https://doi.org/10.1080/15732479.2020.1793208.

[6] D. Konstantinidis, J. M. Kelly, Advances in Low-Cost Seismic Isolation with Rubber, Tenth U.S. National Conference on Earthquake Engineering Frontiers of Earthquake Engineering, 10NCEE, 2014.

[7] A. Khaloo, A. Maghsoudi-Barmi, and M. Ehteshami Moeini, Numerical parametric investigation of hysteretic behavior of steel-reinforced elastomeric bearings under large shear deformation, Structures, 26 (2020), 456-470. https://doi.org/10.1016/j.istruc.2020.04.029

[8] AASHTO, AASHTO LRFD bridge design specifications. Washington, DC: American Association of State Highway and Transportation Officials, 2017.

[9] J. B. Mander, M. J. N. Priestley, and R. Park (1988), Theoretical Stress-Strain Model for Confined Concrete, Journal of Structural Engineering, 114 (1988).

[10] M. Berry, D. E. Lehman, and L. N. Lowes, Lumped-Plasticity Models for Performance Simulation of Bridge Columns. ACI Structural Journal, No. 3 (2008), 270-279.

[11] M.T.A. Chaudhary, M. Abe, and Y. Fujino, Performance evaluation of base-isolated bridge using seismic records. Engineering Structures, 23(2001), 902–910.

[12] B. G. Nielson, Analytical fragility curves for highway bridges in moderate seismic zones, Ph.D. Dissertation, Georgia Institute of Technology, Atlanta, GA, 2005.

[13] Caltrans, Caltrans Structures Seismic Design References, California Department of Transportation, Sacramento, CA, first edition, 1990.

[14] Caltrans, Caltrans Seismic Design Criteria, California Department of Transportation, Sacramento, CA, first edition, 1999.

[15] AASHTO, Design guide specifications for seismic isolation. Washington, DC: American Association of State Highway and Transportation Officials, 2014.

[16] E. Zitzler, M. Laumanns, and S. Bleuler, A tutorial on evolutionary multiobjective optimization. Metaheuristics for

Multiobjective Optimization, Economics and Mathematical Systems, 535 (2004).

[17] O. Lavan and R. Levy, Simple iterative use of Lyapunov's solution for the linear optimal seismic design of passive devices in framed structures, Journal of Earthquake Engineering, 13 (2009), 650–666.

[18] A. Khansefid, and A. Bakhshi, Advanced two-step integrated optimization of actively controlled nonlinear structure under mainshock–aftershock sequences, Journal of Vibration and Control, 25 (2019), 748-62.

[19] A. Khansefid, A. Maghsoudi-Barmi, and A. Bakhshi, Seismic Performance Assessment of Optimally Designed Base Isolation System Under Mainshock-Aftershock Sequences, 8th International Conference on Seismology and Earthquake Engineering (SEE8), Tehran, Iran, 2019.

[20] M. Ehrgott, Multiobjective optimization. AI Magazine, 29(2008), 47–57.

[21] A. Konak, D. W. Coit, and A. E. Smith, Multi-objective optimization using genetic algorithms: A tutorial. Reliability Engineering & System Safety, 91(92006), 992–1007.

[22] N. Quttineh, Models and methods f or costly global optimization and military decision support systems, PhD Dissertation, Linkoping University, Sweden, 2012.

[23] Caltrans, Bridge Memo to Designers, California Department of Transportation, Sacramento, CA, first edition, 1994.

[24] A.H.M.M. Billah, and M. S. Alam, Seismic fragility assessment of highway bridges: a state-of-the-art review, Structure and Infrastructure Engineering, 11 (2014), 804-832.

[25] K. Mackie, and B. Stojadinovic, Fragility basis for California highway overpass bridge seismic decision making, (PEER Report 2005/02), Pacific Earthquake Engineering Research Center. Berkeley, CA: University of California, 2005.

[26] J. E. Padgett, and R. DesRoches, Methodology for the development of analytical fragility curves for retrofitted bridges, Earthquake Engineering and Structural Dynamics, 37 (2008), 157–174.

[27] A. R. Bhuiyan, and M. S. Alam, Seismic vulnerability assessment of a multi-span continuous highway bridge fitted with shape memory alloy bar and laminated rubber bearing. Earthquake Spectra, 28 (2012), 1379– 1404.

[28] HAZUS, Multi-Hazard Loss Estimation Methodology: Earthquake Model HAZUS-MH MR5 Technical Manual. Washington, DC: Federal Emergency Management Agency, 2020.

[29] E. Choi, R. DesRoches, and B. G. Nielson, Seismic fragility of typical bridges in moderate seismic zones. Engineering Structures, 26 (2004), 187–199.

[30] J. Zhang, and Y. Huo, Evaluating effectiveness and optimum design of isolation devices for highway bridges using the fragility function method. Engineering Structures, 31 (2009), 1648–1660.

[31] F. Naeim, J. M. Kelly, Design of seismic isolated structures: From theory to practice. NY: John Wiley & Sons, 1999.

[32] A. Khansefid, Lifetime risk-based seismic performance assessment of structures equipped with different passive vibration control systems under probable mainshock-aftershock scenarios, Structural Control and Health Monitoring, Under Peer Review, 2020.

[33] L. Danciu, K. Sesetyan, M. Demircioglu, M. Erdik, & D. Giardini, OpenQuake input files of the Seismogenic Source model of the 2014 earthquake model of the Middle East (EMME-Project), 2016.

[34] A. Khansefid, & A. Bakhshi, New model for simulating random synthetic stochastic earthquake scenarios, Journal of Earthquake Engineering, 1-18, 2019.

[35] A. Khansefid, A. Bakhshi, & A. Ansari, Empirical predictive model for generating synthetic non-stationary stochastic accelerogram of the Iranian plateau: including far- and near-field effects as well as mainshock and aftershock categorization. Bulletin of Earthquake Engineering 17:3681–3708, 2019.

[36] A. Maghsoudi-Barmi, Experimental and Numerical Investigation of Laminated Elastomeric Bearings Used as Seismic Base-Isolator Considering Long Term Loading Effects, Doctoral dissertation, Sharif University of Technology, 2020.